



**Microfluidic Single-Cell Analysis of Oxidative Stress in  
*Dictyostelium discoideum***

Journal:	<i>Analyst</i>
Manuscript ID	AN-ART-04-2018-000752.R2
Article Type:	Paper
Date Submitted by the Author:	18-Jun-2018
Complete List of Authors:	Rodogiannis, Kathy; Trinity College, Chemistry Duong, Jessica; Trinity College, Chemistry Kovarik, Michelle; Trinity College, Chemistry



Journal Name

ARTICLE

## Microfluidic Single-Cell Analysis of Oxidative Stress in *Dictyostelium discoideum*

Kathy Rodogiannis,<sup>a</sup> Jessica T. Duong<sup>a</sup> and Michelle L. Kovarik<sup>\*a</sup>Received 00th January 20xx,  
Accepted 00th January 20xx

DOI: 10.1039/x0xx00000x

[www.rsc.org/](http://www.rsc.org/)

Microfluidic chemical cytometry is a powerful technique for examining chemical contents of individual cells, but applications have focused on cells from multicellular organisms, especially mammals. We demonstrate the first use of microfluidic chemical cytometry to examine a unicellular organism, the social amoeba *Dictyostelium discoideum*. We used the reactive oxygen species indicator dichlorodihydrofluorescein diacetate to report on oxidative stress and controlled for variations in indicator loading and retention using carboxyfluorescein diacetate as an internal standard. After optimizing indicator concentration, we investigated the effect of peroxide treatment through single-cell measurements of 353 individual cells. The peak area ratio of dichlorofluorescein to carboxyfluorescein increased from  $1.69 \pm 0.89$  for untreated cells to  $5.19 \pm 2.72$  for cells treated with 40 mM hydrogen peroxide. Interestingly, the variance of the data also increased with oxidative stress. While preliminary, these results are consistent with the hypothesis that heterogeneous stress responses in unicellular organisms may be adaptive.

### Introduction

As scientific interest in cellular heterogeneity has grown, so has the number of methods available for single-cell analysis. Well-established single-cell analysis methods include microscopy and flow cytometry, and single-cell sequencing of both genomic DNA and RNA has recently become more common. Chemical cytometry, which involves the separation and detection of cell contents after cell lysis, complements these methods. Chemical cytometry is based on microelectrophoretic separations, which are well-suited to single-cell analysis.<sup>1,2</sup> Capillary and microchip electrophoresis are compatible with volume-limited samples, can be coupled with highly sensitive fluorescence detection, and provide accurate, multi-analyte quantitation. Microchip electrophoresis has the added advantage of potential automation of other analytical steps on a single device.

To date, microfluidic chemical cytometry has been applied exclusively to individual cells from multicellular organisms. With few exceptions,<sup>3–6</sup> these studies have focused on mammalian cell types, especially leukemia cell lines,<sup>7–15</sup> neuron-like PC-12 cells,<sup>16–19</sup> liver cancer cells (HepG2),<sup>20–23</sup> and red blood cells.<sup>24–27</sup> However, this technology could prove uniquely useful for studying unicellular organisms. Similar to cells from multicellular organisms, these microbes can exhibit varying phenotypes, behavior, and fates despite genetic uniformity. Cellular heterogeneity may play different biological roles in single-cell organisms than it does within the tissues of

multicellular organisms. The use of single-cell analysis of stress response in unicellular organisms is particularly intriguing; biological noise in stress response phenotypes has been hypothesized to be adaptive by allowing a single population to sample a range of responses to an environmental stressor or insult.<sup>28,29</sup>

While cells experience a wide range of stressors, oxidative stress is ubiquitous because reactive oxygen species are generated as byproducts of aerobic cellular respiration. Incomplete reduction of molecular oxygen results in the formation of reactive oxygen species (ROS), such as superoxide radical anion ( $O_2^{\cdot-}$ ), hydrogen peroxide ( $H_2O_2$ ), hydroxyl radicals ( $OH^{\cdot}$ ), and ozone ( $O_3$ ).<sup>30</sup> To mitigate the harmful effects of ROS, aerobic cells have defense mechanisms, including enzymatic defenses (e.g., superoxide dismutase and catalase) and small molecule antioxidants (e.g., glutathione and ascorbic acid). When ROS concentrations overwhelm these defense mechanisms in a cell, oxidative stress occurs. Several chemical cytometry studies have measured cellular concentrations of glutathione, a readily-detected tripeptide that acts as an electron donor to maintain redox homeostasis.<sup>20,21,24–26,31–33</sup> Early studies focused primarily on proof-of-principle device operation and examined small numbers of cells (~10–80 cells per study) that are insufficient for statistical characterization of population-level heterogeneity. As single-cell analysis technologies have matured, studies have investigated larger sample sizes or larger numbers of analytes, including nitric oxide and superoxide anion levels in hundreds of single immune or PC-12 cells<sup>7,34</sup> and 76 different metabolites and lipids in oxidatively-stressed hepatocytes.<sup>35</sup> As with most chemical cytometry experiments, these studies have assayed mammalian cells.

<sup>a</sup> Department of Chemistry, Trinity College, 300 Summit St. Hartford, CT 06106

<sup>b</sup> \*michelle.kovarik@trincoll.edu

In this work, we demonstrate the first application of microfluidic chemical cytometry to a unicellular organism and investigate a biological hypothesis that could not be interrogated by ensemble measurements or traditional single-cell analysis techniques, such as microscopy or flow cytometry. We have developed an assay to investigate the effect of exogenous oxidative stress on the heterogeneity of ROS levels in the social amoeba *Dictyostelium discoideum*, a unicellular eukaryote that is commonly used as a model to study cell migration, differentiation, and chemotaxis.<sup>36</sup> Previous research has shown that *D. discoideum* cells use ROS in cell signaling and are generally robust to oxidative stress.<sup>37–40</sup> In this study, we determined the necessary conditions to use fluorogenic dyes and microfluidic chemical cytometry to measure variation in ROS levels in statistically-relevant numbers of individual *D. discoideum* cells and then compared populations of untreated cells and cells treated with hydrogen peroxide.

## Methods

### Cell culture and dye loading

*D. discoideum* cells from the KAX-3 cell line (DBS0236487, Dicty Stock Center, Northwestern University, Chicago, IL) were cultured in HL-5 medium (14 g/L proteose peptone, 7 g/L yeast extract, 3.5 mM Na<sub>2</sub>HPO<sub>4</sub> and 11 mM KH<sub>2</sub>PO<sub>4</sub> at pH 6.5).<sup>41</sup> The cells were grown in suspension at room temperature with shaking at 180 rpm. Cell density was measured using a hemocytometer and maintained between 5,000 and 5 × 10<sup>6</sup> cells/mL.

For dye loading, the diacetate forms of each dye were mixed in low-fluorescence axenic medium (5 g/L casein peptone, 11 g/L glucose, 0.5 mM NH<sub>4</sub>Cl, 0.2 mM MgCl<sub>2</sub>, 10 μM CaCl<sub>2</sub>, 13 μM EDTA, 13 μM ZnSO<sub>4</sub>·H<sub>2</sub>O, 18 μM H<sub>3</sub>BO<sub>3</sub>, 2.6 μM MnCl<sub>2</sub>·4H<sub>2</sub>O, 0.7 μM CoCl<sub>2</sub>·6H<sub>2</sub>O, 0.6 μM CuSO<sub>4</sub>·5H<sub>2</sub>O, 81 nM (NH<sub>4</sub>)<sub>6</sub>Mo<sub>7</sub>O<sub>24</sub>·4H<sub>2</sub>O, and 5 mM dibasic potassium phosphate, pH 6.5)<sup>42</sup> supplemented with 5 mM probenecid to inhibit export of the anionic dyes from the cells.<sup>43</sup> When used to grow *D. discoideum*, this medium typically contains 50 μM FeCl<sub>3</sub>, which we omitted to avoid iron-catalyzed decomposition of hydrogen peroxide. Cells were incubated with the dyes for 20 min in the dark at room temperature and were subsequently washed and resuspended in low-fluorescence axenic medium containing 5 mM probenecid.

### Plate reader experiments

Dye retention curves were constructed to identify a suitable internal standard. Cells were incubated with 20 μM 2',7'-dichlorodihydrofluorescein diacetate (DCFH<sub>2</sub>DA), carboxyfluorescein diacetate (CFDA), or fluorescein diacetate as described above. An equal number of control cells were incubated without dye. Cells were loaded into 384-well bottom-read, tissue-culture treated plates (Corning) at a density of 2 million cells per well. Fluorescence was measured on a SpectraMax M4 plate reader (Microdevices) using the following

settings: excitation wavelength of 485 nm, emission wavelength of 516 nm, emission cutoff of 515 nm, and medium gain. The retention of each dye over time was determined by measuring fluorescence at 0, 10, 20, 40, 60, and 90 min after loading.

Fluorescence measurements were also made using a plate reader to determine the optimum concentration of DCFH<sub>2</sub>DA needed to measure basal levels of oxidative stress and the optimum concentration of hydrogen peroxide to induce a detectable increase above this basal level. To determine the optimum peroxide concentration, cells were loaded with 20 μM DCFH<sub>2</sub>DA and then resuspended in serial dilutions of hydrogen peroxide in low-fluorescence axenic medium containing 5 mM probenecid for 10 min. To determine the optimum DCFH<sub>2</sub>DA concentration, untreated cells were loaded with 0–500 μM DCFH<sub>2</sub>DA. For both experiments, the resulting dichlorofluorescein (DCF) fluorescence was measured using a plate reader under the conditions described above.

### Microchip fabrication

The microfluidic device was fabricated using standard photolithography and soft lithography procedures.<sup>44</sup> SU-8 2015 photoresist (Microchem) was spun to a thickness of ~20 μm on a 4" silicon wafer by spinning at 2000 rpm for 30 s after an initial spread cycle. The wafer was then baked at 95 °C on a hot plate for 5 min, exposed to ultraviolet light (150 mJ/cm<sup>2</sup>, OAI model 200 mask aligner) through a transparency photomask (32,000 dpi, Fineline Imaging), hard baked for 4 min at 95 °C on a hot plate, developed for 2 min in SU-8 developer, and post-exposure baked for 65 min. For soft lithography, a 10:1 mixture of Sylgard 184 PDMS prepolymer and curing agent was mixed and degassed under vacuum, poured over the SU-8 master, and then cured for 30 min on a hot plate until firm. Access holes were made using a 1-mm biopsy punch, and the PDMS was irreversibly sealed to a cover glass using plasma oxidation. Silicone tubing reservoirs (Masterflex #EW-96440-16) were also plasma-sealed to the device. To reduce cell adhesion and suppress electroosmotic flow, the channels were coated with a supported lipid bilayer of egg phosphatidylcholine. This coating formed spontaneously upon filling the channels with small unilamellar vesicles that were prepared by sonication, as described previously.<sup>45</sup>

### Microchip operation

For microchip experiments, cells were labeled with 200 μM DCFH<sub>2</sub>DA<sub>4</sub> and 200 μM CFDA as described above. After dye loading, cells were washed and resuspended in low-fluorescence medium containing 5 mM probenecid. Treated cells were incubated with 8 or 40 mM hydrogen peroxide for 10 min. (The peroxide stock concentration was estimated by UV absorbance.) After washing, cells were resuspended at a density of 1 million cells/mL in low-fluorescence axenic medium containing 5 mM probenecid and loaded onto the microfluidic device.

The microfluidic device was rinsed with low-fluorescence axenic medium containing 5 mM probenecid, and the flow of cells

through the device was initiated via hydrostatic flow. The cells were lysed in an electric field (300 V/cm) applied via platinum wire electrodes and a high voltage sequencer (LabSmith HVS448LC 3000D). The negatively charged fluorescent products DCF and carboxyfluorescein (CF) were electrophoretically separated in the separation channel and detected by laser-induced fluorescence (LIF) 5 mm below the lysis intersection. For LIF detection, a solid state laser (OBIS LS, 488 nm, 2 mW) was directed into an inverted microscope (Olympus IX73) through a laser filter cube and a 40× objective (0.55 NA) to the microscope stage. The fluorescence emission from the dyes was detected using a photomultiplier tube (Hamamatsu NO: 34950002, control voltage = 0.6), and the resulting signal was processed using a current-to-voltage converter (Hamamatsu C7319) and a tunable active filter (Frequency Devices 900CT/9L8L) with a corner frequency of 10 Hz. The high voltage power supply and data collection were controlled using a custom LabVIEW program (National Instruments 2010), and data analysis was performed using Cutter 7.<sup>46</sup> To account for interday and interdevice variation and to ensure reproducibility, cells were sampled on at least two different days and devices for each treatment group.

## Results and Discussion

For common ROS, including superoxide, peroxide, and nitric oxide, several fluorogenic indicators are available with varying degrees of specificity. We chose to use the generally nonspecific reporter DCFH<sub>2</sub>DA as a global indicator of cellular ROS levels. In cells, esterases remove the acetate groups, and the precursor is oxidized by ROS to produce fluorescent DCF.<sup>47</sup> Past work with DCFH<sub>2</sub>DA has used microscopy or flow cytometry to measure total cellular fluorescence. However, these traditional single-cell techniques are unable to differentiate noisiness in ROS from noisiness in dye uptake, esterase activity, and retention.<sup>47</sup> The separation step of chemical cytometry allowed us to use an internal standard, allowing the noisiness in ROS levels to be differentiated from noise generated by these other processes.

We considered CFDA and fluorescein diacetate as potential internal standards. Both molecules are structurally similar to DCFH<sub>2</sub>DA and become fluorescent upon cleavage of their acetate groups by intracellular esterases. To determine which dye would be the better internal standard, we evaluated the loading and retention of each dye in ensemble populations of cells via fluorescence measurements using a plate reader (Figure 1). The initial fluorescence of cells loaded with fluorescein diacetate was much higher than that of cells loaded with either DCFH<sub>2</sub>DA or CFDA. Retention of the fluorescent dyes after diacetate cleavage was also more similar for DCF and CF compared to fluorescein. Cells loaded with DCFH<sub>2</sub>DA or CFDA had rapid initial declines in fluorescence intensity, which plateaued above the background level for controls cells after ~10 min. In contrast, the fluorescence of cells loaded with fluorescein diacetate did not plateau until after ~40 min but reached a much lower level that was closer to the baseline fluorescence of cells that were not loaded with the indicator.

Fluorescein is less polar than either CF, which contains an additional carboxylic acid group, or DCF, which has polar carbon-chlorine bonds. These structural differences may account for the different loading and retention behaviors of this dye. Based on these results, we selected CFDA as the more suitable internal standard for measurements with DCFH<sub>2</sub>DA.

There are four steps that must occur in order to detect fluorescent DCF from a cell: (1) DCFH<sub>2</sub>DA must be taken up by the cells, (2) esterases must cleave the diacetate groups, (3) the resulting anion must be retained by the cell, and (4) a two-electron oxidation must occur to form the fluorescent DCF product. In order to detect CF from a cell, the first three steps must still occur, but the fourth step (oxidation) is not necessary because CFDA becomes fluorescent upon cleavage of the diacetate groups alone. Consequently, the use of CFDA as an internal standard should account for cell-to-cell variation in (1) uptake, (2) esterase activity, and (3) retention, such that variation in the DCF/CF ratio reflects variation in the oxidation step only.

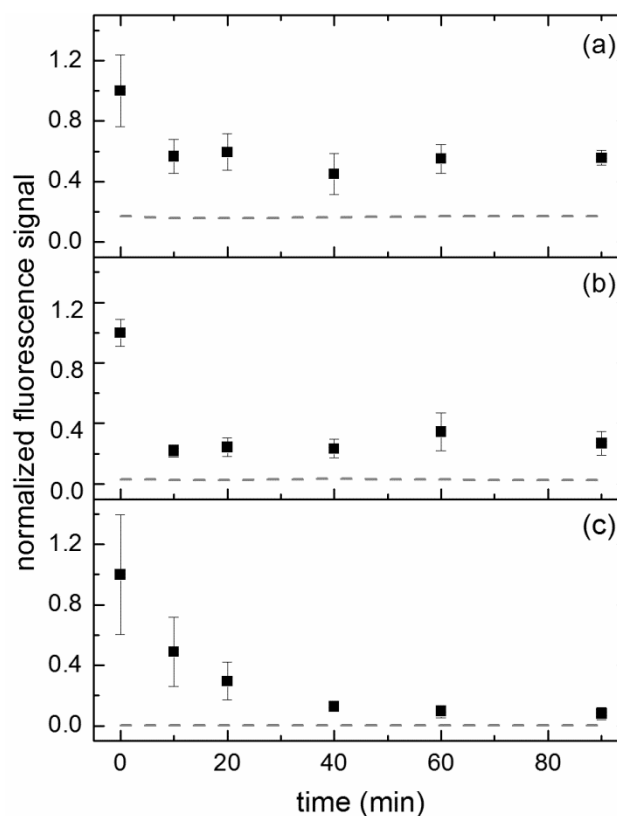


**Figure 1.** Ensemble fluorescence signal over time of cells loaded with 20  $\mu$ M (a) fluorescein diacetate, (b) CFDA, or (c) DCFH<sub>2</sub>DA. Data are normalized to the initial fluorescence, and the dashed gray line shows the average fluorescence of control cells not exposed to DCFH<sub>2</sub>DA. In all panels, error bars represent the standard deviation of  $n = 3$  biological replicates collected on different days.

We also used ensemble fluorescence measurements of cell populations on a plate reader to determine optimum hydrogen peroxide concentrations to induce oxidative stress in *D. discoideum*. *D. discoideum* is substantially more resistant to oxidative stress than mammalian cells,<sup>37</sup> and previous studies have used peroxide concentrations from 0.25–5 mM for

treatment periods of 15 min to 40 h.<sup>39,48–50</sup> To examine acute stress over the time period of dye retention, we tested hydrogen peroxide concentrations from 0–65 mM. Cells were loaded with DCFH<sub>2</sub>DA, resuspended in a peroxide solution for 10 min, washed and measured. Although the peroxide concentrations tested in this study were higher than those used in previous works, the duration of the treatment was shorter and cells were treated in a relatively rich low-fluorescence medium rather than phosphate buffer to minimize osmotic stress. Cells were stained with Trypan blue and phloxine B<sup>48</sup> and were monitored for growth over a 24 h period to confirm that the treated cells remained viable. Increasing peroxide concentration was correlated with higher levels of cell fluorescence and higher variability between biological replicates (Figure 2a). This variation further demonstrated the need for an internal standard to differentiate interday variation in dye loading and retention from variation in ROS levels in cells. For single-cell experiments, we chose to use hydrogen peroxide concentrations of 8 and 40 mM, which produced average fluorescence levels that were 3 and 10 standard deviations above the average fluorescence of untreated cells, respectively.

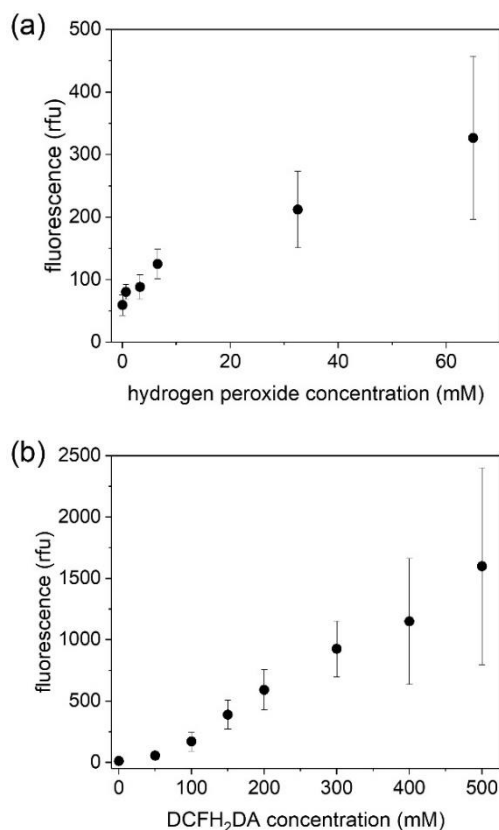


**Figure 2.** (a) Ensemble fluorescence signal for cells loaded with 20  $\mu\text{M}$  DCFH<sub>2</sub>DA and treated with 0–65 mM hydrogen peroxide. Error bars represent the standard deviation for  $n = 5$  biological replicates collected on different days. (b) Ensemble fluorescence signal for cells loaded with varying DCFH<sub>2</sub>DA concentrations. Error bars represent the standard deviation for  $n = 3$  biological replicates collected on different days. Data were collected using a plate reader.

We also optimized the concentration of DCFH<sub>2</sub>DA used to load cells. We tested DCFH<sub>2</sub>DA loading concentrations from 0–500  $\mu\text{M}$  and observed that fluorescence initially increased with concentration non-linearly (Figure 2b). Because DCFH<sub>2</sub> must

compete with endogenous antioxidants to react with ROS, the level of fluorescence is expected to depend not only on ROS concentrations but also on the relative concentrations of DCFH<sub>2</sub> and endogenous ROS. These data suggested that at low concentrations, DCFH<sub>2</sub> levels in the cells were low compared to endogenous antioxidant concentrations such that most ROS reacted with native antioxidants, resulting in minimal DCF fluorescence. As the DCFH<sub>2</sub>DA loading concentration increased, internal DCFH<sub>2</sub> concentrations increased, as did fluorescence. However, the rate of increase was lower at very high loading concentrations. As DCFH<sub>2</sub> levels became very high, the production of the fluorescent DCF product may have been limited by ROS levels. Thus, for subsequent single-cell experiments, we loaded cells using 200  $\mu\text{M}$  DCFH<sub>2</sub>DA to ensure that the indicator dye concentrations were sufficient to produce signal but did not obscure cell-to-cell differences in endogenous antioxidant concentrations.

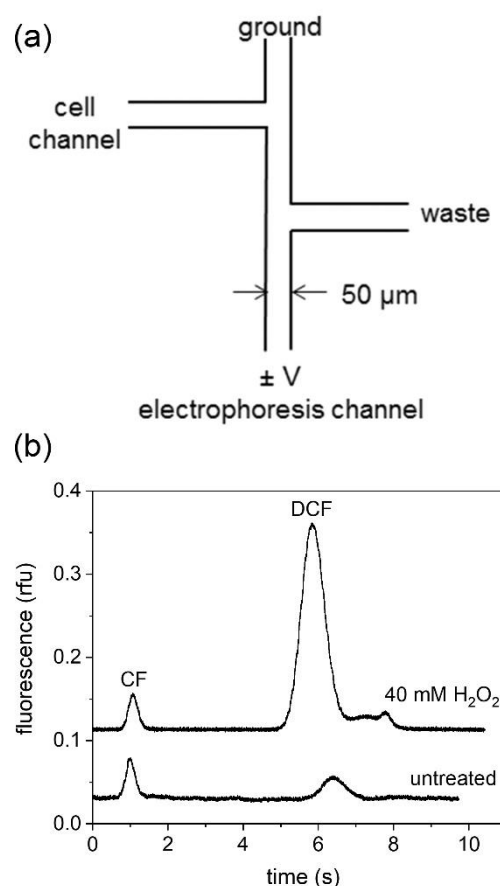


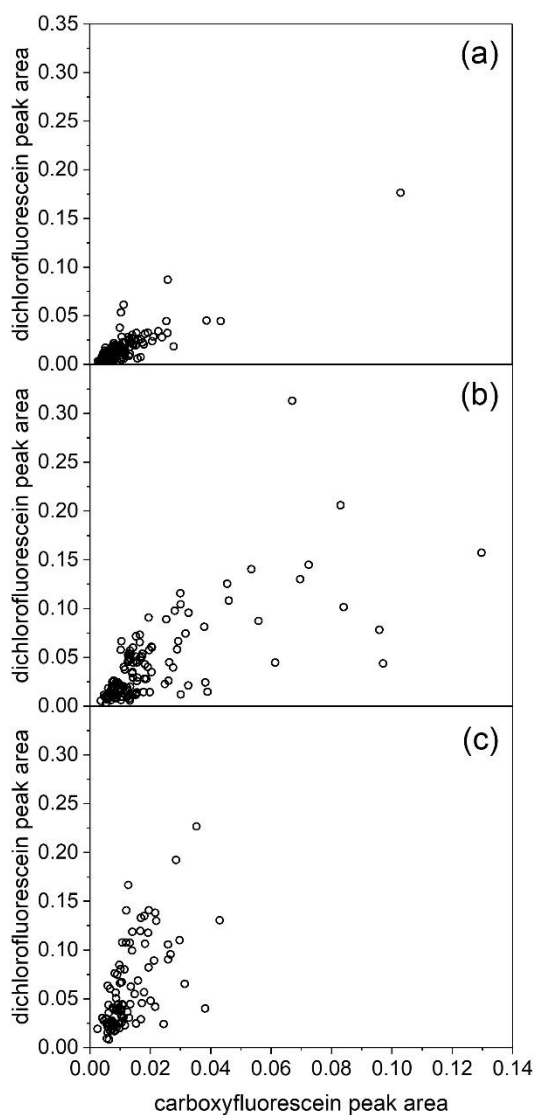
**Figure 3.** (a) Schematic of the microfluidic device and (b) electropherograms of representative individual cells treated with 0 or 40 mM hydrogen peroxide.

After establishing appropriate cell treatment conditions, single-cell measurements by chemical cytometry were conducted using a device adapted from a recent publication (Figure 3a).<sup>7</sup> Cells travelled through the device via hydrostatic flow and were lysed by a 300 V/cm electric field in the vertical channel. Most debris, which had minimal electrophoretic mobility, was carried to the waste reservoir by the hydrostatic flow, while the anionic dyes were electrophoretically separated and detected by laser-

induced fluorescence in the vertical channel, located 5 mm below the intersection with the waste channel. For each lysed cell, peaks were identified based on the relative migration times of DCF and CF standards on a simple cross microchip with the same lipid coating. As expected, under suppressed electroosmotic flow conditions, the two dyes migrated toward the anode, and the more negatively charged CF reached the

that was uncorrelated with the CF peak area as resulting from differences in oxidation of the DCFH<sub>2</sub>, possibly owing to differences in oxidative stress levels between cells.

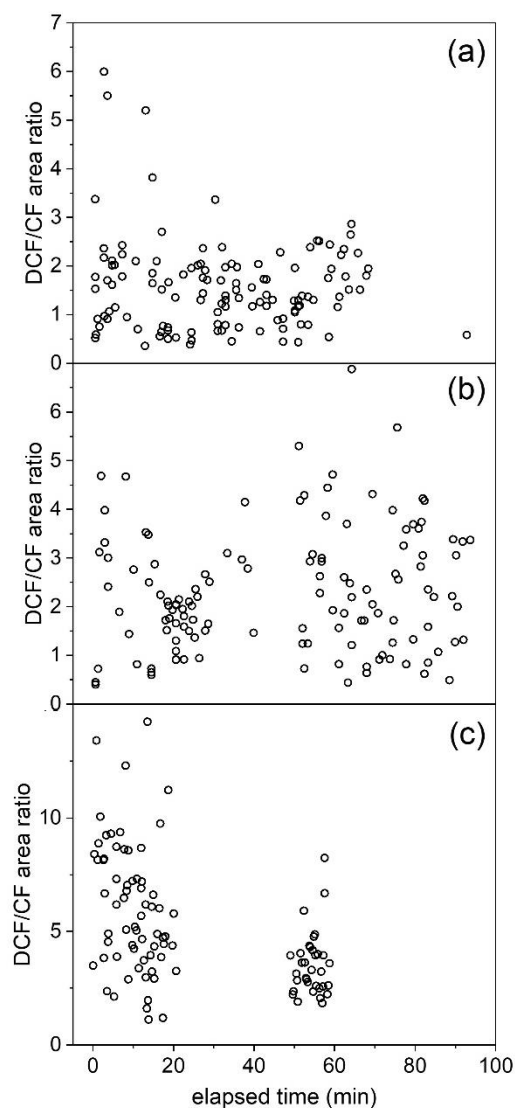
In solution, DCFH<sub>2</sub>DA can undergo auto-oxidation over time,<sup>47</sup> and we considered that cells might accumulate DCF over the course of the experiment via auto-oxidation or ongoing endogenous ROS production. If this were the case, cells analyzed late in an experiment would have higher DCF fluorescence than cells analyzed early in an experiment, artificially broadening the population distribution. To test for time dependence, we plotted the peak area ratios as a function of time and calculated Pearson correlation coefficients for DCF peak area and peak area ratios as a function of time. No trend in peak area ratio as a function of time was observed in the data (Figure 5), and correlation coefficients ranged from -0.47-0.13, suggesting minimal correlation between the time when individual cells were lysed for analysis and their DCF



detector first (Figure 3b).

**Figure 4.** Relationship between dichlorofluorescein (DCF) and carboxyfluorescein (CF) signals for cells treated with (a) 0 mM, (b) 8 mM, or (c) 40 mM hydrogen peroxide. Each point represents a single cell.

For each cell, the CF and DCF peak areas were quantified. When these two values were used as coordinates for individual cells, some correlation was observed (Figure 4). Least squares linear fits to the data resulted in  $R^2$  values for the 0, 8, and 40 mM data sets of 0.59, 0.48, and 0.38, respectively. These results indicated that some of the variation in DCF fluorescence between cells was correlated with variation in the CF signal, implicating external factors, such as cell size, esterase activity, and dye uptake and retention, which would affect the internal standard in similar ways. We interpreted the variation in DCF peak area



fluorescence signal or peak area ratio.

**Figure 5.** Peak area ratio versus time for cells treated with (a) 0 mM, (b) 8 mM, or (c) 40 mM hydrogen peroxide. Each point represents a single cell.

One advantage of single-cell analysis is the opportunity to quantify biological noise within a population. Recent work has hypothesized that heterogeneity in stress responses may be advantageous to single-celled organisms because it allows the population to sample a range of responses.<sup>28,29</sup> To quantify the noisiness of a population, it is necessary to estimate the population standard deviation,  $\sigma$ , from the sample standard deviation,  $s$ , of each group. For small sample sizes (e.g.,  $N < 30$ ),  $s$  is generally a poor estimator of  $\sigma$ . As sample size increases, estimation of  $\sigma$  from  $s$  rapidly improves, then plateaus. This occurs because the distribution of  $s$  values follows a chi square distribution, allowing calculation of the sample size required to obtain a confidence interval of a desired width.<sup>51</sup> At a sample size of 100 cells,  $s$  should be within  $\pm 14\%$  of  $\sigma$  95% of the time. Doubling the sample size to 200 cells only narrows this interval slightly; for  $N = 200$ ,  $s$  is within  $\pm 10\%$  of  $\sigma$  95% of the time. Based on these diminishing returns, we determined that  $N = 100$  cells was a reasonable minimum sample size for each group.

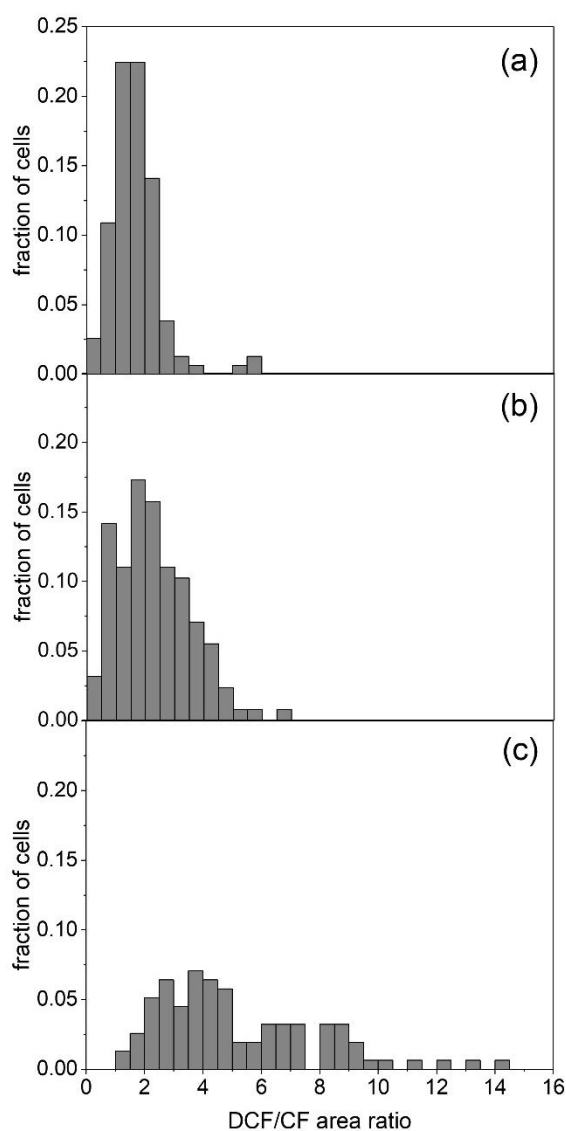


**Figure 6.** Histograms of peak area ratios for (a) untreated control cells ( $N = 125$  individual cells) and cells treated with (b) 8 mM  $\text{H}_2\text{O}_2$  ( $N = 127$  individual cells), and (c) 40 mM  $\text{H}_2\text{O}_2$  ( $N = 101$  individual cells). For each panel, data were pooled from experiments conducted over multiple days and devices.

To extract information concerning the noisiness of ROS levels independent of other processes (e.g., dye uptake, retention, esterase activity, and cell size), the DCF/CF ratio for each cell was used to correct for differences between cells that were correlated with CF intensity. Histograms of these ratios were generated to visualize the population distributions of each treatment group. All distributions were approximately Gaussian with slight tailing toward higher area ratios (Figure 6). As expected, treatment with hydrogen peroxide increased ROS levels in cells, and consequently, the average DCF/CF area ratio for a population (Table 1). Mean values were significantly different between all three groups for the DCF peak area and for the DCF/CF area ratio ( $p < 0.001$  for both tests).

**Table 1.** Statistical characteristics of the untreated and treated cell populations.

		Untreated	8 mM $\text{H}_2\text{O}_2$	40 mM $\text{H}_2\text{O}_2$
		125	127	101
CF Area	<i>N</i>	125	127	101
	median	0.010	0.013	0.010
	average	0.012	0.021	0.013
	standard deviation	0.012	0.021	0.008
	coefficient of variation	102%	102%	61%
DCF Area	median	0.015	0.026	0.041
	average	0.022	0.044	0.058
	standard deviation	0.046	0.046	0.044
	coefficient of variation	208%	104%	75%
DCF/CF Area Ratio	median	1.56	2.05	4.40
	average	1.69	2.29	5.19
	standard deviation	0.89	1.25	2.72
	coefficient of variation	53%	55%	52%

The variance of the treated populations,  $\sigma^2$ , also increased upon treatment, as shown by the wider distribution of peroxide-treated cells relative to untreated cells (Figure 6 and Table 1). Using a Brown-Forsythe test, we determined that the variances of the DCF/CF ratio distributions were significantly different for the three treatment groups ( $p < 0.001$ ). The treated populations exhibited a wider range of ROS levels, suggesting a range of capacities of individual cells to resist oxidative stress. Although the absolute variation (represented by the standard deviation) increased with peroxide treatment, the relative variation (represented by the coefficient of variation) remained relatively constant (Table 1) and was within the range previously reported for similar measurements using a fluorescein-based nitric oxide reporter in Jurkat cells.<sup>7</sup> Further work is needed to establish whether this trend holds true for other sources and levels of oxidative stress.

## Conclusions

We have established an optimized experimental design for single-cell measurements of oxidative stress in *D. discoideum*. While still preliminary, these data coincide with the hypothesis that heterogeneity in stress responses may be adaptive in unicellular organisms, such as *D. discoideum*. Further studies should elucidate the biological underpinnings of this heterogeneity by examining the effects of the source and

concentration of ROS, as well as the roles of cell cycle, catalase expression, and mitochondrial function. These results are also the first chemical cytometry data for *D. discoideum*, an important model organism for studies of cell migration, chemotaxis, and differentiation.<sup>36</sup> The unique social life cycle of this organism makes it a particularly interesting model for single-cell studies, and the ability to adapt a microfluidic chemical cytometry device developed for human cells to an evolutionarily distant eukaryote underscores the broad applicability of this technology.<sup>7</sup>

## Conflicts of interest

There are no conflicts to declare.

## Acknowledgements

The authors thank Casey Crowley for initial work optimizing the probenecid treatment; Lhacene Adnane and Prof. Helena Silva at the University of Connecticut Nanofabrication Facility and Julia Clapis for assistance with photolithography; and Prof. Brooks Emerick for helpful discussions. This material is based upon work supported by the National Science Foundation under RUI grant no. MCB-161548, by Trinity College, and by a Cottrell Scholar Award to MLK from Research Corporation for Science Advancement.

## Notes and references

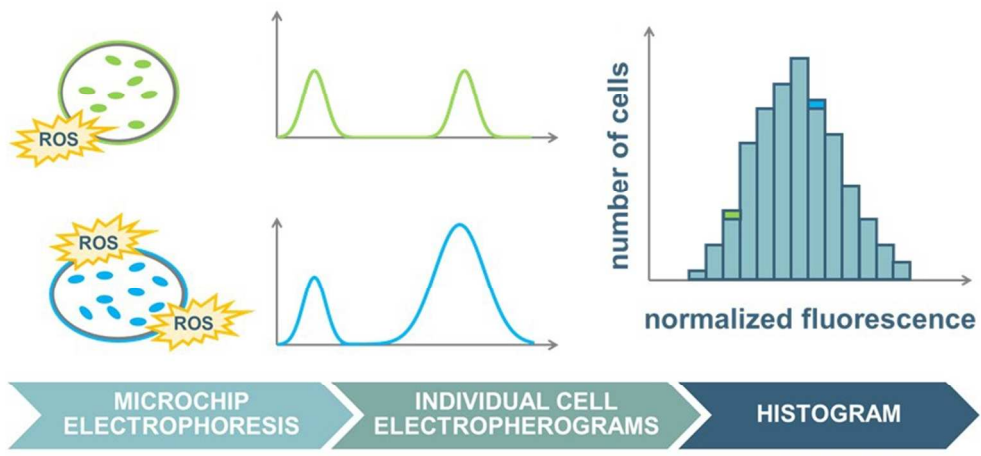
- C. E. Sims and N. L. Allbritton, *Lab Chip*, 2007, **7**, 423–440.
- L. M. Borland, S. Kottegoda, K. S. Phillips and N. L. Allbritton, *Annu. Rev. Anal. Chem.*, 2008, **1**, 191–227.
- F. Xia, W. Jin, X. Yin and Z. Fang, *J. Chromatogr. A*, 2005, **1063**, 227–233.
- Hellmich Wibke, Pelargus Christoph, Leffhalm Kai, Ros Alexandra and Anselmetti Dario, *Electrophoresis*, 2005, **26**, 3689–3696.
- W. Hellmich, D. Greif, C. Pelargus, D. Anselmetti and A. Ros, *J. Chromatogr. A*, 2006, **1130**, 195–200.
- D. Greif, L. Galla, A. Ros and D. Anselmetti, *J. Chromatogr. A*, 2008, **1206**, 83–88.
- E. C. Metto, K. Evans, P. Barney, A. H. Culbertson, D. B. Gunasekara, G. Caruso, M. K. Hulvey, J. A. Fracassi da Silva, S. M. Lunte and C. T. Culbertson, *Anal. Chem.*, 2013, **85**, 10188–10195.
- M. A. McClain, C. T. Culbertson, S. C. Jacobson, N. L. Allbritton, C. E. Sims and J. M. Ramsey, *Anal. Chem.*, 2003, **75**, 5646–5655.
- N. R. Munce, J. Li, P. R. Herman and L. Lilje, *Anal. Chem.*, 2004, **76**, 4983–4989.
- H. Wu, A. Wheeler and R. N. Zare, *Proc. Natl. Acad. Sci. U. S. A.*, 2004, **101**, 12809–12813.
- B. Deng, Y. Tian, X. Yu, J. Song, F. Guo, Y. Xiao and Z. Zhang, *Anal. Chim. Acta*, 2014, **820**, 104–111.
- M. L. Kovarik, A. J. Dickinson, P. Roy, R. A. Poonnen, J. P. Fine and N. L. Allbritton, *Integr. Biol.*, 2014, **6**, 164–174.
- M. L. Kovarik, P. K. Shah, P. M. Armistead and N. L. Allbritton, *Anal. Chem.*, 2013, **85**, 4991–4997.
- D. E. W. Patabadige, J. Sadeghi, M. Kalubowilage, S. H. Bossmann, A. H. Culbertson, H. Latifi and C. T. Culbertson, *Anal. Chem.*, 2016, **88**, 9920–9925.
- D. E. W. Patabadige, T. Mickleburgh, L. Ferris, G. Brummer, A. H. Culbertson and C. T. Culbertson, *Electrophoresis*, 2016, **37**, 1337–1344.
- Li Xiangtang, Zhao Shulin and Liu Yi-Ming, *ChemistrySelect*, 2016, **1**, 5554–5560.
- X. Li, S. Zhao, H. Hu and Y.-M. Liu, *J. Chromatogr. A*, 2016, **1451**, 156–163.
- Q. Li, P. Chen, Y. Fan, X. Wang, K. Xu, L. Li and B. Tang, *Anal. Chem.*, 2016, **88**, 8610–8616.
- L. Li, Y. Fan, Q. Li, R. Sheng, H. Si, J. Fang, L. Tong and B. Tang, *Anal. Chem.*, 2017, **89**, 4559–4565.
- S. Yue and Y. Xue-Feng, *J. Chromatogr. A*, 2006, **1117**, 228–233.
- C. Xu, M. Wang and X. Yin, *Analyst*, 2011, **136**, 3877–3883.
- Y. Sun, M. Lu, X.-F. Yin and X.-G. Gong, *J. Chromatogr. A*, 2006, **1135**, 109–114.
- L. F. Cheow, A. Sarkar, S. Koltz, D. Lauffenburger and J. Han, *Anal. Chem.*, 2014, **86**, 7455–7462.
- J. Gao, X.-F. Yin and Z.-L. Fang, *Lab Chip*, 2004, **4**, 47–52.
- S. Zhao, X. Li and Y.-M. Liu, *Anal. Chem.*, 2009, **81**, 3873–3878.
- C.-X. Xu and X.-F. Yin, *J. Chromatogr. A*, 2011, **1218**, 726–732.
- J. S. Mellors, K. Jorabchi, L. M. Smith and J. M. Ramsey, *Anal. Chem.*, 2010, **82**, 967–973.
- J. R. S. Newman, S. Ghaemmaghami, J. Ihmels, D. K. Breslow, M. Noble, J. L. DeRisi and J. S. Weissman, *Nature*, 2006, **441**, 840–846.
- D. J. Wilkinson, *Nat. Rev. Genet.*, 2009, **10**, 122–133.
- K. Krumova and G. Cosa, in *Singlet Oxygen: Applications in Biosciences and Nanosciences*, ed. S. Nonell and C. Flors, 2016, **1**, 1–21.
- B. L. Hogan and E. S. Yeung, *Anal. Chem.*, 1992, **64**, 2841–2845.
- N. Gao, L. Li, Z. Shi, X. Zhang and W. Jin, *Electrophoresis*, 2007, **28**, 3966–3975.
- M. Hao, C. Li, R. Liu and M. Jing, *Spectrochim. Acta. A. Mol. Biomol. Spectrosc.*, 2015, **149**, 600–606.
- L. Li, Q. Li, P. Chen, Z. Li, Z. Chen and B. Tang, *Anal. Chem.*, 2016, **88**, 930–936.
- L. Zhang and A. Vertes, *Anal. Chem.*, 2015, **87**, 10397–10405.
- S. J. Annesley and P. R. Fisher, *Mol. Cell. Biochem.*, 2009, **329**, 73–91.
- B. Katoch and R. Begum, *J. Biosci.*, 2003, **28**, 581–588.
- Y. P. Tao, T. P. Misko, A. C. Howlett and C. Klein, *Dev. Camb. Engl.*, 1997, **124**, 3587–3595.
- C.-H. Choi, B.-J. Kim, S.-Y. Jeong, C.-H. Lee, J.-S. Kim, S.-J. Park, H.-S. Yim and S.-O. Kang, *Dev. Biol.*, 2006, **295**, 523–533.
- G. Bloomfield and C. Pears, *J. Cell Sci.*, 2003, **116**, 3387–3397.
- P. Fey, A. S. Kowal, P. Gaudet, K. E. Pilcher and R. L. Chisholm, *Nat. Protoc.*, 2007, **2**, 1307–1316.
- H. MacWilliams, Low Fluorescence Axenic Medium, [http://dictybase.org/techniques/media/lowflo\\_medium.html](http://dictybase.org/techniques/media/lowflo_medium.html), (accessed 5 June 2017).
- R. Furukawa, J. E. Wampler and M. Fechheimer, *J. Cell Biol.*, 1988, **107**, 2541–2549.
- D. C. Duffy, J. C. McDonald, O. J. Schueller and G. M. Whitesides, *Anal. Chem.*, 1998, **70**, 4974–4984.
- K. S. Phillips, S. Kottegoda, K. M. Kang, C. E. Sims and N. L. Allbritton, *Anal. Chem.*, 2008, **80**, 9756–9762.
- J. G. Shackman, C. J. Watson and R. T. Kennedy, *J. Chromatogr. A*, 2004, **1040**, 273–282.
- X. Chen, Z. Zhong, Z. Xu, L. Chen and Y. Wang, *Free Radic. Res.*, 2010, **44**, 587–604.
- M. X. U. Garcia, C. Foote, S. van Es, P. N. Devreotes, S. Alexander and H. Alexander, *Biochim. Biophys. Acta BBA - Gene Struct. Expr.*, 2000, **1492**, 295–310.
- A. Taminato, R. Bagattini, R. Gorjão, G. Chen, A. Kuspa and G. M. Souza, *Mol. Biol. Cell*, 2002, **13**, 2266–2275.

## ARTICLE

Journal Name

- 1  
2  
3 50 S. Veeranki, S.-H. Hwang, T. Sun, B. Kim and L. Kim, *Dev. Biol.*,  
4 2011, **360**, 351–357.  
5 51 L. Laurencell and Francois A Dupuis, in *Statistical Tables,*  
6 *Explained and Applied*, World Scientific Publishing, Singapore,  
7 2002, p. 245.  
8  
9  
10  
11  
12  
13  
14  
15  
16  
17  
18  
19  
20  
21  
22  
23  
24  
25  
26  
27  
28  
29  
30  
31  
32  
33  
34  
35  
36  
37  
38  
39  
40  
41  
42  
43  
44  
45  
46  
47  
48  
49  
50  
51  
52  
53  
54  
55  
56  
57  
58  
59  
60

1  
2  
3  
4  
5  
6  
7  
8  
9  
10  
11  
12  
13  
14  
15  
16  
17  
18  
19  
20  
21  
22  
23  
24  
25  
26  
27  
28  
29  
30  
31  
32  
33  
34  
35  
36  
37  
38  
39  
40  
41  
42  
43  
44  
45  
46  
47  
48  
49  
50  
51  
52  
53  
54  
55  
56  
57  
58  
59  
60



79x38mm (300 x 300 DPI)